

# Development of an individualized biomechanical knee model for calculation of the tibiofemoral force during isokinetic knee extension

Martyna BIAŁECKA<sup>1</sup> , Jacek BUŚKIEWICZ<sup>1</sup> , Tomasz WALCZAK<sup>1</sup> , Tomasz PIONTEK<sup>2</sup> ,  
Monika GRYGOROWICZ<sup>3</sup> 

<sup>1</sup> Poznan University of Technology, Institute of Applied Mechanics, Faculty of Mechanical Engineering, Poland,

<sup>2</sup> Poznan University of Medical Sciences, Department of Spine Disorders and Paediatric Orthopaedics, Poland; Rehasport Clinic FIFA Medical Centre of Excellence, Department of Orthopaedic Surgery, Poland,

<sup>3</sup> Poznan University of Medical Sciences, Department of Physiotherapy, Poland; Rehasport Clinic FIFA Medical Centre of Excellence, Department of Sport Science, Poland

**Corresponding author:** Martyna BIAŁECKA, email: martyna.bialecka@put.poznan.pl

**Abstract** Meniscus injuries are increasingly being treated using arthroscopic surgical techniques, and isokinetic measurement is commonly used to assess return of knee joint function. Accurate estimation of tissue loading in the knee joint requires the use of models tailored to the gender of the patient, as anatomical differences between men and women have previously been shown to affect the results of similar studies. This paper describes developing the model to analyse knee loads among patients with meniscus injuries treated with a novel surgical technique. Personalized patient data were collected from their knee magnetic resonance imaging scans and knee isokinetic measurements performed at 60 deg/s angular velocity. The knee joint loads estimated with the model proposed in this work demonstrated higher compressive forces in the knee joint, indicating the need for greater caution when using isokinetic measurements safely after meniscus-save arthroscopy surgery.

**Keywords:** isokinetic test, magnetic resonance imaging, meniscus injury.

## 1. Introduction

Since it is well established that meniscectomy is associated with early degenerative osteoarthritis, meniscal repair procedures are suggested whenever possible. Different strategies for meniscus suturing have been described, including all-inside arthroscopic augmentation techniques for meniscal repair that demonstrated to be safe and can offer an additional tool to save the meniscus in patients otherwise scheduled for meniscal removal [1].

Advances in rehabilitative techniques have also been observed in patients with meniscal injuries. Currently, isokinetic evaluation is one of the standard assessments of the requirements that the patient must meet to qualify for the next stage of phase-based rehabilitation protocols, especially when more active and strength-required exercises will be introduced [2]. However, during the isokinetic test (IT), the forces acting on the knee joint are very high due to the high external loads applied to the limb and the low movement angular velocity [3], so it is necessary to optimally calculate the forces that actually act on the patient's joint during isokinetic movement and to try to relate the peak torques recorded during the isokinetic test to the forces acting on the joint during activities of daily living, such as walking or jumping.

Several models were developed to assess knee loads and calculate tibiofemoral and shear forces, including three-dimensional FEM (finite element method) models [4], in vitro cadaver models, models driven by EMG (electromyography) [5–7] and analytical models [8–10]. Analytical models, like the one presented in current study, are the least expensive and the least time-consuming techniques to apply in everyday practice [11].

Unfortunately, previously published models have some limitations: for example, they neither take into account the measurements from MRI scans nor include up-to-date knowledge regarding displacement of the point of contact between the tibia and femur, and the angular orientation of the patellar tendon [9, 10, 12, 13]. Since now it is possible to individualize the biomechanical model based on the patient's MRI scan, it is necessary to update the analytical models. The prime reason is that it might affect the magnitude of the forces calculated using the analytical model and the instants of their occurrence.

Therefore, we developed and verified an analytical novel personalized mechanical model to predict the magnitude of the knee tibiofemoral and shear forces. The developed model aims to reformulate the conditions under which an isokinetic test can be performed to assess the rehabilitation process of patients treated due to medial meniscus tears. The current model overcomes limitations previously described and was adjusted to the sex of the patient, as it has previously been proven that anatomical differences between men and women affect the results of similar studies [14]. Since the current model will be applied for the analysis of knee loads in a group of meniscal injury patients treated with a novel operative technique that performs the biomechanical evaluation as a standard assessment, we verified it for the concentric isokinetic movement of knee extension.

## 2. Methods

The model developed in this study was verified in a group of six patients (3 male, 3 females, mean values and standard deviation – aged  $45.7 \pm 3.7$  years, weight  $77.7 \pm 16.9$  kg, and height  $175.2 \pm 4.5$  cm) treated for a medial meniscus tear, without lateral meniscus lesions, according to the surgical technique presented by Piontek et al. [15], one year after arthroscopy. This procedure is a standard approach in Rehasport Clinic FIFA Medical Centre of Excellence in Poznan, Poland [1], therefore we verified knee loads after this particular surgical procedure. All data were collected retrospectively from a sample of previously conducted studies approved by the Bioethics Committee of the Medical University of Poznan [1, 15].

### 2.1. Model concept

We developed the model based on data from the MRI scans and the raw IT data. Combining them, we calculated the tibiofemoral force throughout the ROM (range of motion) of knee isokinetic extension based on muscle torque measured on an isokinetic dynamometer. The model is called TFITIMD (Tibiofemoral Force Isokinetic Test Individual MRI Data). To calculate the tibiofemoral forces, we formulated a two-dimensional mechanical model of the shank and tibial articular surface during isokinetic knee extension. We expanded the model presented by Masouros [16] and analysed the movement in the sagittal plane only. The shank displacement is a function of the knee extension angle. The extension was defined as a change in angle between the tibial long axis and femur long axis from  $90^\circ$  (starting position) to  $180^\circ$  (extended knee), performed in a sitting position with a constant angular velocity of  $60^\circ/\text{s}$  and measured with an isokinetic dynamometer. TFITIMD model is presented in Fig. 1, where  $XZ$  and  $xz$  denotes stationary and movable coordinate systems, respectively, where the  $x$  axis defines the tibial plateau and  $z$  axis (perpendicular to the  $x$ ) passes through the centroid of the proximal tibia cortical bone outline found in the MRI transversal plane. The characteristic points of the model, especially places where the key forces for the model are applied are described in the Fig. 1. The main forces applied to the model are:  $F$  – the force exerted by the isokinetic dynamometer lever on the lower leg preventing limb acceleration,  $F_{TF}$  – the reaction force between the femur and tibia (assumed as perpendicular to the  $x$ ),  $F_S$  – the reaction force between the femur and tibia (shear force, parallel to the  $x$ ),  $F_{PT}$  – the force acting in the patellar tendon,  $Q$  – the weight of the shank and tibia. Angles marked in Fig. 1 are:  $\varphi$  – knee extension angle,  $\beta(\varphi)$  – the angle between the tibial long axis ( $l_{kp}$ ) and the direction of the patellar tendon as a function of  $\varphi$  calculated using the data from a previous study [17] and measurements made on MRI scans (see Eqs. (1) – (3)),  $\alpha$  – the angle between  $l_{kp}$  and the  $z$  axis, measured for the extended knee based on the MRI image,  $\lambda_0$  – the angle between the tibial long axis and the vertical direction ( $Z$  axis of the global immovable coordinate system),  $\gamma_0$  – the angle between the tibial plateau and the horizontal direction ( $X$  axis of the global immovable coordinate system);  $\lambda_0$  and  $\gamma_0$  were measured individually for each patient in the final position (extended knee) based on the MRI scans.  $l_{kp}$  is the tibial long axis's connecting point  $S$  with the centre of the ankle; it can be designated according to a previous study [17] in which the tibial long axis was localised in the sagittal plane as a line parallel to the posterior wall of the tibial shaft, passing through the middle of the tibial spines. Two-dimensional models of the knee joint do not take into account the screw-home motion (SHM) involving the external rotation of the tibia relative to the femur during the final stages of knee extension. The SHM contributes to knee stability by tightening the cruciate ligaments, particularly during activities such as gait and squatting. This tightening increases the forces in these ligaments, which, in consequence, affects the reaction forces in the knee joint. The SHM is most significant during the last 20 degrees of knee extension [18, 19].

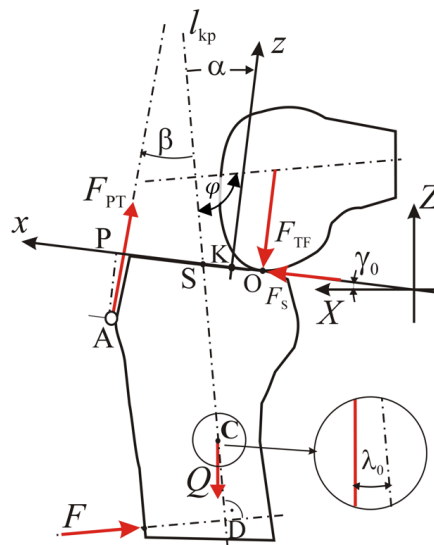


**Figure 1.** The model of the knee joint during extension on an isokinetic dynamometer in the starting position ( $\varphi = 90^\circ$ ). A – patellar tendon attachment, C – the centre of mass for the shank and tibia segment, D – the intersection of the direction of force  $F$  with the tibial long axis, O – the movable point of contact between tibial and femur articular surfaces, P – the projection of a patellar tendon attachment on the x axis, S – the centre of the tibial plateau (the intersection of the tibial long axis with the x axis), K – the geometric centre of the tibial outline in the first transverse plane fully under the cartilage on MRI scan,  $l_{kp}$  – the tibial long axis.

**2.2. Measurements based on MRI scans**

Distances essential to the model were measured based on T1-weighted time spin echo unilateral MRI scans of operated knee joints, with resolution of  $384 \times 384$  px and layers spaced 3 mm apart, made in the sagittal, coronal and transversal planes. To introduce the coordinate system in the tibia, we applied the methodology presented by Beynnon et al. [20] (Fig. 2). The DICOM images were viewed and analysed using free software Onis 2.5.

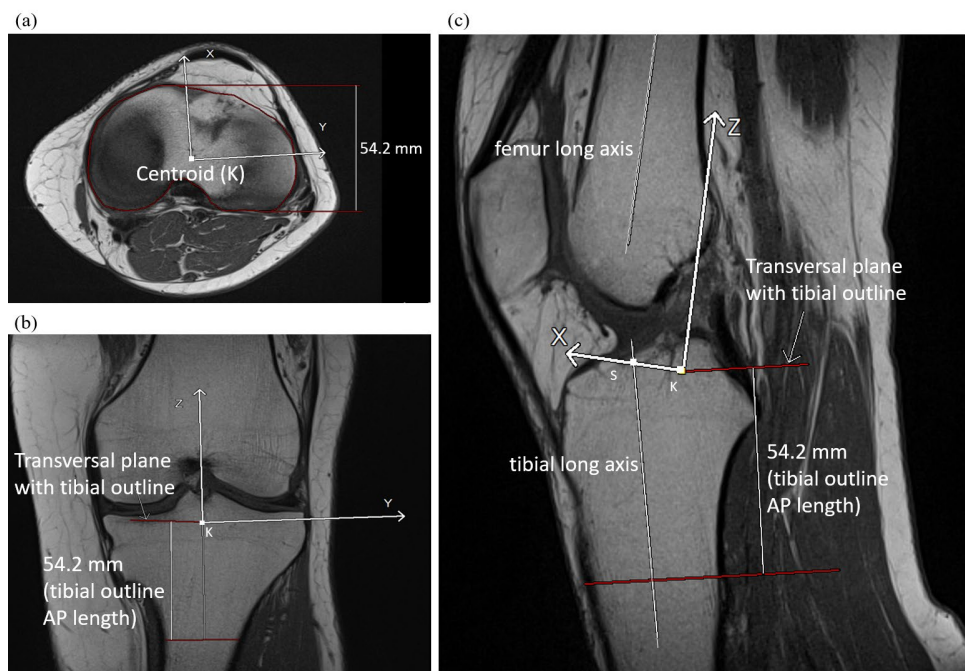


**Figure 2.** Coordinate system in MRI image according to the applied methodology.

### 2.3. Measurements based on isokinetic tests

Data for IT analysis was collected from the knee isokinetic raw data of each patient. Three repetitions of knee isokinetic flexion-extension movements were performed in concentric–concentric mode at 60°/s. The measurements were performed at the clinic, according to the test procedures presented in a previous study [21]. The raw data from those evaluations were exported to a text file. Subsequently, data were imported to MATLAB software and filtered with third-order lowpass IIR filter, passband frequency of 0.1 Hz and with compensation for frequency-dependent delay.

### 2.4. Model description

The model was developed to analyse a rotation of the shank and foot where the thigh is a stationary solid. The shank is a rigid body with symmetric mass distribution around the tibial long axis, where the centre of mass is located on the tibial long axis. The location of the point of contact between tibia and femur (point O) changed during knee extension and its location was calculated based on empirical studies from the literature [22]. The centre of mass of the shank and foot (point C) is located 44.16% and 44.59% along the longitudinal length of the tibia, calculated from the axis of the knee joint for females and males, respectively (distance  $d_{SC}$ , between the  $x$  axis and the point C) [23]. The weight of the shank and foot was marked as  $Q$ ; the mass of the shank and foot was calculated as 6.1% and 5.7% of the body mass for females and males, respectively [23]. The extension of the knee joint is caused by the force exerted by the patellar tendon  $F_{PT}$ , acting pointwise on the tuberosity of the tibia, which is the patellar tendon attachment (point A). The lever of the isokinetic dynamometer acts on the shank with force  $F$  applied pointwise perpendicular to the tibial long axis.  $F$  can be calculated based on the torque registered by the dynamometer and the distance between the knee's axis of rotation and the point at which force  $F$  is applied (knee attachment/lever of the isokinetic dynamometer is fixed proximally to the medial malleoli). The force acting on the tibial articular surface has two components: the force normal to the tibial articular surface ( $F_{TF}$ ) and the shear force ( $F_S$ ) that is assumed to be parallel to the tibial articular surface. Due to the very low coefficient of friction (ranging from 0.01 to 0.09 [24]) the friction forces occurring in the knee joint are small, therefore  $F_S$  mainly represents the forces acting in the cruciate ligaments [25].

In order to determine the value of  $\beta$  (Fig. 1) for every knee flexion angle  $\varphi$ , we applied a second-order polynomial approximation to the results presented in the study of Varadarajan et al. [17] for the sagittal plane angle measured for the central part of the patellar tendon. Based on that, we formulated two equations, which estimate the value of angle  $\beta$  throughout the ROM during knee extension:

$$M_{mod}(\varphi) = -0.0011 \cdot \varphi^2 + 0.54 \cdot \varphi - 43, \quad (1)$$

where  $M_{mod}$  is the sagittal plane angle for the central part of the patellar tendon among men expressed in degrees,  $\varphi$  is the knee flexion angle.

$$W_{mod}(\varphi) = -0.00125 \cdot \varphi^2 + 0.62 \cdot \varphi - 48.5, \quad (2)$$

where  $W_{mod}$  is the sagittal plane angle for the central part of the patellar tendon among women expressed in degrees,  $\varphi$  is the knee flexion angle.

In order to adjust the values of angle  $\beta$  to the individual anatomy of the patient, two values were measured on the MRI scans,  $\beta_{mri}$  and  $\varphi_{mri}$ . The value of  $\beta(\varphi)$  was calculated as follows:

$$\beta(\varphi) = M_{mod}(\varphi) + (\beta_{mri} - M_{mod}(\varphi_{mri}))\left(\frac{\varphi}{180^\circ}\right), \quad (3)$$

where  $\beta_{mri}$  is the angle between  $l_{kp}$  and the patellar tendon and  $\varphi_{mri}$  is the angle between  $l_{kp}$  and the femur long axis in the position presented in the MRI image. All angles were expressed in degrees.

Most of the distances essential to the model, like PS and AP, were constant during movement and were measured for the extended knee directly on the MRI image. Distances, like  $d_{SC}$  and  $d_{SO}$ , were varying during knee extension. The distance  $d_{SD}$  between the  $x$  axis (tibial articular surface) and the position at which force  $F$  is applied to the shank by the lever of the isokinetic dynamometer measured in the direction of the  $z$  axis was calculated based on the height of the patient and data presented in the study [26], where the tibial length (from the malleolar tip to the lateral condyle) was calculated based on patient's height.  $d_{SO}$  is the distance between the  $l_{kp}$  axis and the point of contact between the tibia and femur (point O), measured in the direction of the  $x$  axis. The distance can take positive and negative values and changes with knee flexion, due to movement of point O (the  $x$  coordinate of point S is constant).

Displacement of the contact point during knee extension is very similar on the medial and lateral condyles within the knee extension range of 90° to 180° [22]. In order to determine the value of

displacement of the contact point for every knee flexion angle  $c(\varphi)$ , we applied a second-order polynomial approximation to the measurements for the medial condyle presented by Qi et al. [22].

It was assumed that the extreme position of the contact point (position for the extended knee) is located 6% along the anterior–posterior length of the tibia, in the anterior direction (positive direction of the  $x$  axis) from the origin of the coordinate system. 6% is the average location of this point on the medial and lateral condyles [22].

To calculate  $d_{SO}$  we applied the results of the study [22] and the measurements performed on the MRI image, then:

$$d_{SO} = x_{Smri} - x_o(\varphi) \text{ [mm]}, \tag{4}$$

$$x_o(\varphi) = x_{Of} - c(\varphi) \text{ [mm]}, \tag{5}$$

where  $x_{Smri}$  is the  $x$  coordinate of point S, measured directly on the MRI image and  $x_{Of}$  is the  $x$  coordinate of point O in the extreme position, calculated as 6% of the anterior–posterior length of the tibia.  $c(\varphi)$  is the displacement of point O:

$$c(\varphi) = -0.00051 \cdot \varphi^2 + 0.038 \cdot \varphi + 10.5 \text{ [mm]}. \tag{6}$$

### 2.5. Formulation of equations

The torque measured by the isokinetic dynamometer was balanced by the torque exerted by the patellar tendon attached to the tuberosity of the tibia, so that the movement of the shank and foot has a constant angular speed. We formulated the dynamic equation for the movement of the shank and foot centre of mass (point C):

$$m \vec{a}_c = \vec{F} + \vec{Q} + \vec{F}_{TF} + \vec{F}_S + \vec{F}_{PT} \tag{7}$$

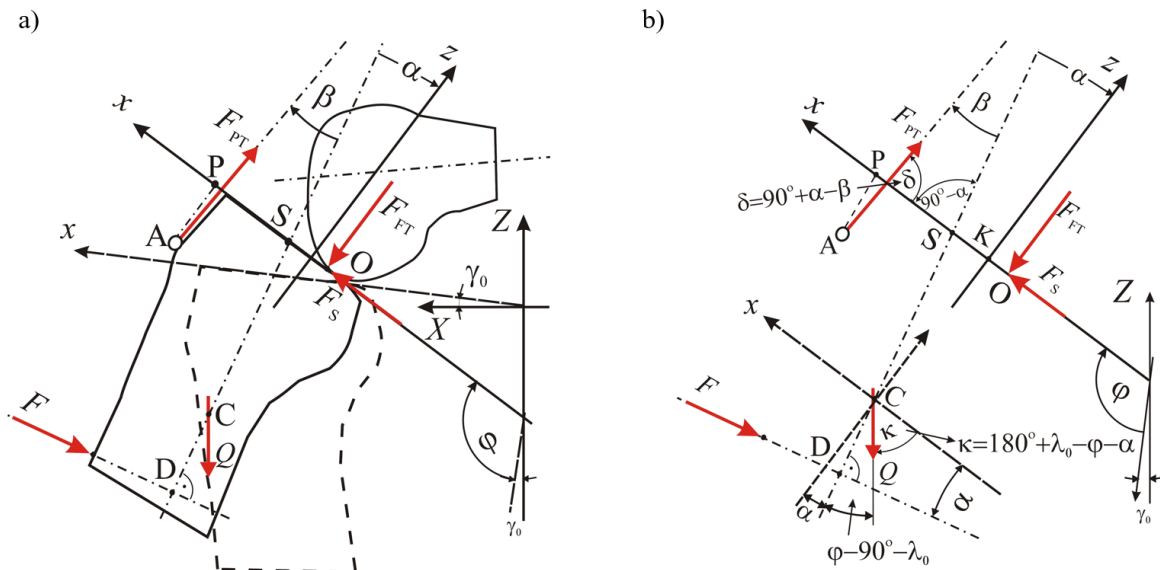


**Figure 3.** Illustration for: a) the equations determination for the knee flexed by the  $\varphi$  angle, b) angles calculation for knee flexed by the  $\varphi$  angle.

During extension of the knee from the starting position, the angular relations and the values of forces presented in Fig. 1 and Fig. 3 are functions of angle  $\varphi$ . Those changes were included in the motion equations.

The angular momentum equation for rotational motion was formulated as follows:

$$J_C \frac{d^2\varphi}{dt^2} = M_C = M_S + |\vec{SC} \times m \vec{a}_c|, \tag{8}$$

where  $J_C$  is the mass moment of inertia of the shank and foot with respect to the foot and shank mass centre C, and  $m$  is the mass of the foot and shank.

It was verified that the term  $m\overline{a}_C$  is negligibly small compared to other forces (and nearly parallel to segment CS). Moreover, if the angular velocity is constant in the IT, then angular acceleration vanishes. The moment of forces with respect to point S (centre of tibial plateau) is computed since this point is well defined and can be precisely localised on MRI scans. The following forces can be derived from Eqs. (7) and (8):

$$F_{TF} = (F \cdot |d_{SD}| + F \cdot |PS| \cdot \sin(\alpha) - mg \cdot |PS| \cdot \sin(\kappa) - mg \cdot |d_{SC}| \cdot \sin(\lambda - \varphi + 90^\circ) + F \cdot |AP| \cdot \sin(\alpha) \cdot \text{tg}(\alpha - \beta) - mg \cdot |AP| \cdot \sin(\kappa) \cdot \text{tg}(\alpha - \beta)) \cdot \frac{1}{d_{SO} - |PS| - |AP| \cdot \text{tg}(\alpha - \beta)}, \quad (9)$$

$$F_S = (-F \cdot |d_{SD}| + |AP| \cdot (F \cdot \cos(\alpha) + mg \cdot \cos(\kappa)) + |PS| \cdot (F \cdot \cos(\alpha) + mg \cdot \cos(\kappa)) \cdot \text{ctg}(\alpha - \beta) - F \cdot d_{SO} \cdot \cos(\beta) \cdot \frac{1}{\sin(\alpha - \beta)} - mg \cdot d_{SO} \cdot \cos(\alpha - \beta + \kappa) \cdot \frac{1}{\sin(\alpha - \beta)} + mg \cdot d_{SC} \cdot \sin(\lambda - (\varphi - 90^\circ))) \cdot \frac{1}{|AP| + (|PS| - d_{SO}) \cdot \text{ctg}(\alpha - \beta)}. \quad (10)$$

## 2.6. The verification procedures and data analysis

Shear and tibiofemoral forces calculated with TFITMD were compared to forces calculated with the model previously described by Nisell et al. [10] and widely applied in the estimation of joint forces during knee ITs (referred to as Nisell's model) (Fig. 4). Four parameters were verified: tibiofemoral peak force ( $F_{TF}$ ), shear peak force ( $F_S$ ), angle at peak of tibiofemoral force ( $A_{TF}$ ) and angle at peak of shear tibiofemoral force ( $A_S$ ). Tibiofemoral and shear peak forces were expressed in [N] and in relation to the body weight [BW]; angles were presented in degrees. Descriptive statistics of these parameters were calculated. Normality of distribution of the parameters was verified using the Shapiro–Wilk test. To verify our model, we analysed whether there were any differences between values of forces and angles calculated with TFITMD and Nisell's model. The differences were tested with the Student's t-test for independent samples or with the Mann–Whitney U, when Levene's test (analysing the equality of variances of the analysed parameter) was statistically significant. PQStat 1.6.2. statistical program was used for all statistical analysis, and the significance level  $\alpha$  was assumed at 0.05.

## 3. Results

Only for predicted absolute  $F_{TF}$ , predicted  $A_{TF}$ , absolute  $F_S$  we cannot reject the hypothesis that the distribution of the parameter aligns to normal distribution (the  $p$ -value is larger than  $\alpha$ ) (Tab. 1).

Values of absolute and relative tibiofemoral knee forces predicted with our model were significantly higher when compared to values calculated using the Nisell model (mean difference for absolute  $F_{TF}$  was 432.04 N,  $p = 0.026$ , and mean difference for relative  $F_{TF}$  was 0.594 BW,  $p = 0.047$ , respectively). Levene's test confirmed a violation of the assumption of equal variances for predicted absolute  $F_S$  and predicted  $A_S$  (Tab. 2). Absolute shear forces were significantly higher when predicted with our than Nisell's model (mean difference for absolute  $F_S$  was 124.75 N,  $p = 0.017$ ). Although our model also predicted higher knee relative shear force, no significant differences were noted when compared to the Nisell's model (mean difference for relative  $F_S$  was 0.15 BW,  $p = 0.093$ ). When comparing the angle at which the peak torque occurs, it can be noted that for tibiofemoral normal and shear forces the peak appear later and earlier, respectively if the prediction was done with our model. However, these observations were not confirmed to be statistically significant.

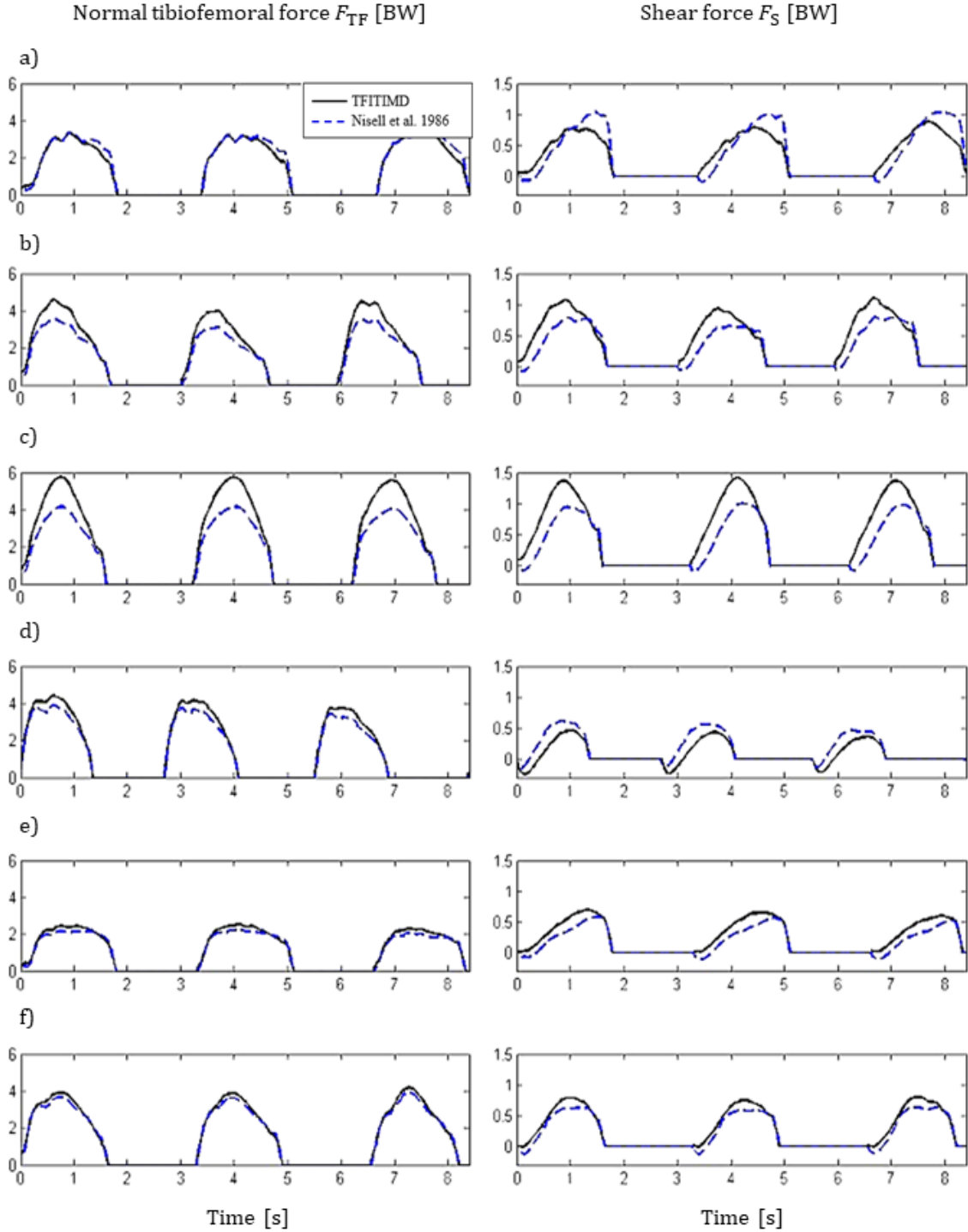


**Figure 4.** Normal (left) and shear (right) tibiofemoral force during three isokinetic knee extensions calculated with the model developed in the current study (TFITMD) and with Nisell model adjusted for this study. Three top graphs (a – c) present data for women, three bottom graphs (d – f) present data for men. Zero force values between first and second and second and third knee extension represent the time when a patient performed knee flexions, applicable for neither presented nor Nisell model.

**Table 1.** Absolute and relative values of calculated peak normal ( $F_{TF}$ ) and shear ( $F_S$ ) tibiofemoral force, their occurrence at extension angle reported as mean (standard deviation) for three test repetitions. Data for model presented in this study (TFITIMD) and for model adapted from Nisell et al [10].

	Peak torque [Nm]	Peak torque [Nm/kg]	Force Prediction Model	$F_{TF}$ [N]	$F_{TF}$ [BW]	$A_{TF}$ [°]	$F_S$ [N]	$F_S$ [BW]	$A_S$ [°]
Mean (SD)	111.31 (28.22)	1.42 (0.27)	Current study	2970 (625)	3.93 (1.04)	132 (6.83)	666 (162)	0.889 (0.310)	150 (10.7)
			Nisell et al.	2538 (475)	3.34 (0.646)	128 (12.3)	545 (67.9)	0.739 (0.197)	156 (15.5)
IQR	94.7	0.87	Current study	946	1.03	5.17	247	0.325	11.6
			Nisell et al.	498	0.625	10.5	115	0.375	28.3
Min-Max	76.72-171.42	0.94-1.81	Current study	1966-4089	2.20-5.70	119-149	379-915	0.400-1.50	134-173
			Nisell et al.	1964-3592	2.00-4.10	106-162	431-647	0.500-1.00	137-177
Shapiro-Wilk W	0.893	0.945	Current study	0.970	0.944	0.935	0.963	0.923	0.942
			Nisell et al.	0.902	0.865	0.897	0.935	0.834	0.840
Shapiro-Wilk p	0.043	0.349	Current study	0.807	0.339	0.238	0.669	0.147	0.311
			Nisell et al.	0.063	0.015	0.052	0.235	0.005	0.006

**Table 2.** Between-model comparison for all predicted values.

	Test <sup>b,c</sup>	Statistic	df	p	Mean difference	SE difference	Statistic measure	Effect Size	Lower 95% <sup>d</sup>	Upper 95% <sup>d</sup>
$F_{TF}$ [N]	t	2.34	34.0	0.026	432.044	184.961	Cohen's d	0.779	0.066	1.472
$F_{TF}$ [BW]	t	2.06	34.0	0.047	0.594	0.288	Cohen's d	0.688	-0.013	1.371
$A_{TF}$ [°]	t	1.16	34.0	0.253	3.850	3.308	Cohen's d	0.388	-0.283	1.048
$F_S$ [N] <sup>a</sup>	U	87.0	NA	0.017	124.750	NA	Rank biserial correlation	0.463	NA	NA
$F_S$ [BW]	t	1.73	34.0	0.093	0.150	0.087	Cohen's d	0.577	-0.112	1.250
$A_S$ [°] <sup>a</sup>	U	132.5	NA	0.359	-4.213	NA	Rank biserial correlation	0.182	NA	NA

<sup>a</sup> Levene's test is significant ( $p < .05$ ), suggesting a violation of the assumption of equal variances

<sup>b</sup> Student's t

<sup>c</sup> Mann-Whitney U

<sup>d</sup> 95% confidence interval

#### 4. Discussion

The presented approach allows the calculation of the tibiofemoral force in the entire ROM available in IT in an individualised way. Distances measured on MRIs, which is an individualised feature, were used in the model, while two parameters ( $\beta$  and  $d_{SO}$ ) were averaged for the bigger group based on fluoroscopic studies. Thus, TFITIMD allows the estimation of tibiofemoral force based on data usually collected in the treatment process, like the muscle torque measured in knee IT, static MRI scan of the extended knee, and basic patient features (height and body mass). Another advantage is the simplicity and low cost of the model, since every step is reproducible with freely available software. Previous models do not analyse interindividual features that affect forces acting in the knee [12, 27, 28] or use optimization methods and specialized software [9], [27, 29], making them difficult to apply in everyday practice. Furthermore, the TFITIMD model differentiates the calculations according to the sex of the patient ( $\beta$ ,  $d_{SD}$  distance and MRI measurements are sex-specific), unlike the previous studies [12, 27].

The results of our study show that IT at 60°/s for patients, especially in the early postoperative period, should be carefully discussed, as patients treated due to meniscus lesions can generate high muscle torques (up to  $1.38 \pm 0.68$  Nm/kg [30]) as soon as 4 weeks postoperatively. These torque values are comparable to the values achieved by patients analysed in the current study 12 months postoperatively ( $1.42 \pm 0.27$  Nm/kg, Tab. 1). The main component of the tibiofemoral force is normal to the tibial plateau, distributed mainly in the tibia. The peak normal force calculated in our study is relatively high (up to 5.7 BW, Tab. 1) compared to other activities of daily living (ADL) described in the literature (level walking: 2.7–4.3 BW, stair climbing: 4.4 BW [31], body weight squat: up to 3.64 BW) [32] or measured in vivo with instrumented knee prostheses (level walking: 2.5 BW, stair climbing: 3.2 BW, skiing: up to 5 BW [33]). The possible reason for the high values of the normal component of the tibiofemoral force is the specificity of the isokinetic test, which requires the generation of maximum muscle forces ( $\vec{F}_{PT}$ ) on short lever arms. The lever arm in the TFITIMD model is represented by the  $d_{SO} + |PS|$  distance (Fig. 1, Eq. 4-5). Such a scenario rarely occurs in loads observed during everyday activities. Despite this, the isokinetic test remains the most commonly used to examine muscle strength and its safe use should be considered from a biomechanics perspective, especially among operated patients.

As shown in the current study, peak shear forces are much lower than normal forces, but they are carried by less durable knee structures, mainly cruciate ligaments that provide resistance to the anterior and posterior translation of the tibia relative to the femur. The ultimate load of the femur–ACL–tibia complex is  $2160 \pm 157$  N as reported by Woo et al. based on cadaver studies [34]. The shear forces calculated in our study are close to those presented in studies [9, 12], however, they are higher than those reported for ADL using similar models [35] or measured in vivo with instrumented knee prostheses (level walking: 0.4–0.5 BW [31], rise from a chair: 0.1–0.3 or playing tennis:  $0.28 \pm 0.12$  BW [33]). Even if the shear forces are much lower than the normal forces, they should be considered during the early rehabilitation process of patients after ACL reconstruction, since it should be noted that after surgery the strength of the graft is much lower than that of a healthy ligament. Estimating the limit loads for grafts is still difficult, and it is one of the challenges for in vitro or mathematical modelling research. However, values indicated by mathematical models, are sensitive to the arm length for the moment of the muscle torque [36]; therefore any comparison of the obtained data might be difficult.

TFITIMD was verified based on the model published previously by Nisell et al. [10], with respect to the similarity of the models. The simplicity of the Nisell's model makes it the most possible to apply in everyday clinical practice. The main differences between these two models are: (1) the source of data used to make the anthropometrical measurements (MRI scan vs. measurements made on cadaver knees and radiographic study of healthy volunteers) and (2) the source of data used to estimate a change in two variables: displacement of the point of contact between the tibia and femur, and the angle between the tibial long axis ( $l_{kp}$ ) and the direction of the patellar tendon (literature data from fluoroscopic studies vs. measurements made on radiograms). Normal and shear tibiofemoral forces were calculated using the two models for the same set of data. Statistically significant differences were observed between model outcomes for peak normal tibiofemoral force, calculated as the absolute and relative value ( $p = 0.026$  and  $p = 0.047$ , respectively; Tab. 2) and the absolute shear force ( $p = 0.017$ ; Tab. 2). Although our model also predicted higher knee relative shear force when compared to the Nisell's model, no significant differences were noted ( $p = 0.093$ ).

These results suggest that individual anthropometric features measured on MRI scans are important in estimating knee intraarticular force. We observed that the maximum normal forces appear in the first 50° of knee extension (mean  $A_{TF}$   $132^\circ \pm 6^\circ$ , whereas the peak shear force is reached for higher knee extension angles (mean  $A_S$   $150 \pm 11^\circ$ , according to TFITIMD, Tab. 1). The mean  $A_S$  angle calculated by TFITIMD was lower than in Nisell's model (mean angle  $155^\circ \pm 15^\circ$ , Tab. 1). This observation may be relevant to determine safe ROM in IT among patients with ACL reconstruction, because it is recommended not to overload the ACL in the early postoperative period [37]. Limiting extension movement to 140° could prevent the development of excessive shear forces during the IT, and thus improve patient safety during test.

Apart from the main strengths of our study – the simplicity of TFITIMD and its individualization – it also has a few limitations. The model is applicable only to isokinetic knee extension. However, previous studies have shown that isokinetic knee extensions at 60°/s generate knee forces approximately two times higher than those for knee flexion [9]. Hence, we focus our modelling on knee extension, since it should be analysed while ensuring patient safety. Another limitation is that the cruciate ligaments are not included in the model and we neglected the effects of friction between the femur and the tibia. Similarly to previously published papers [29, 32] it is assumed that the shear force during knee extension is the force acting in ACL, as force parallel to the tibial articular surface, and that the coefficient of friction is negligible in human joints. This

approach seems to be reasonable because the ACL provides 86% of the total restraining force to the anterior drawer [38]. Another limitation is that the distance between the articular surface of the tibia and the attachment of the dynamometer to the shank ( $d_{SD}$ ) was calculated based on the height of the patient and literature data. This was caused by the retrospective character of this study and the lack of actual data on this distance. Moreover, a brief commentary on the limitations of two-dimensional modelling and the omission of the SHM is advisable. The forces in the cruciate ligaments generated by the SHM increase the values of the joint forces, as do the forces in the antagonistic muscles (not included in the model either). This effect may not be as significant during isometric exercise, where the maximum forces are reached for the angles less than the last 20° of knee extension. Nevertheless, confirmation of this fact requires the use of a three-dimensional model.

We developed and verified a two-dimensional mechanical model that uses two inputs: muscle torque and geometric measurements from knee MRI scan, to calculate normal and shear tibiofemoral forces. This fills the gap among similar models currently available in the literature because it allows the calculation of tibiofemoral force in an individualized way using MRI scans, data from up-to-date fluoroscopic studies, and differentiate model parameters according to the patient's sex. Based on the results of this study, it is our recommendation to avoid peak intraarticular forces in the knee joint, especially in the case of patients in the early postoperative period. To avoid high forces during isokinetic knee extensions, a ROM not exceeding 50° is recommended. Alternatively, the test should be performed at a higher velocity than 60°/s, as the forces acting in the knee joint in isokinetic knee testing decrease with the test speed, according to Hill's law [12].

### Acknowledgments

M. B. thanks Rehasport Clinic Ltd, for providing data for this study. While carrying out this research, M. B. was supported with grant 0612/SBAD/3641, and J. B. and T. W. were supported with grant 0612/SBAD/3640, both grants allocated by the Ministry of Education and Science in Poland.

### Additional information

The authors declare: no competing financial interests and that all material taken from other sources (including their own published works) is clearly cited and that appropriate permits are obtained.

### References

1. T. Piontek et al.; Complex Meniscus Tears Treated with Collagen Matrix Wrapping and Bone Marrow Blood Injection: A 2-Year Clinical Follow-Up; *Cartilage*, 2016, 7(2), 123–139; DOI: 10.1177/1947603515608988
2. J. T. Cavanaugh, S. E. Killian; Rehabilitation following meniscal repair; *Curr. Rev. Musculoskelet. Med.*, 2012, 5(1), 46–58; DOI: 10.1007/s12178-011-9110-y
3. F. Serpas, T. Yanagawa, M. Pandy; Forward-dynamics Simulation of Anterior Cruciate Ligament Forces Developed During Isokinetic Dynamometry; *Comput. Methods Biomech. Biomed. Engin.*, 2002, 5(1), 33–43; DOI: 10.1080/1025584021000001614
4. A. Schmitz, D. Piovesan; Development of an Open-Source, Discrete Element Knee Model; *IEEE Trans. Biomed. Eng.*, 2016, 63(10), 2056–2067; DOI: 10.1109/TBME.2016.2585926
5. B. L. S. Bedo, D. S. Catelli, M. Lamontagne, P. R. P. Santiago; A custom musculoskeletal model for estimation of medial and lateral tibiofemoral contact forces during tasks with high knee and hip flexions; *Comput. Methods Biomech. Biomed. Engin.*, 2020, 23(10), 658–663; DOI: 10.1080/10255842.2020.1757662
6. A. Falisse, S. Van Rossom, I. Jonkers, F. De Groote; EMG-Driven Optimal Estimation of Subject-SPECIFIC Hill Model Muscle–Tendon Parameters of the Knee Joint Actuators; *IEEE Trans. Biomed. Eng.*, 2017, 64(9), 2253–2262; DOI: 10.1109/TBME.2016.2630009
7. A. Szpala, A. Rutkowska-Kucharska, M. Stawiany; Symmetry of electromechanical delay, peak torque and rate of force development in knee flexors and extensors in female and male subjects; *Acta Bioeng. Biomech.*, 2015, 17(1), 61–68; DOI: 10.5277/ABB-00103-2014-01
8. A. Geier, H. Aschemann, D. D'Lima, C. Woernle, R. Bader; Force Closure Mechanism Modeling for Musculoskeletal Multibody Simulation; *IEEE Trans. Biomed. Eng.*, 2018, 65(11), 2471–2482; DOI: 10.1109/TBME.2018.2800293

9. K. R. Kaufman, K. N. An, W. J. Litchy, B. F. Morrey, E. Y. S. Chao; Dynamic joint forces during knee isokinetic exercise; *Am. J. Sports Med.*, 1991, 19(3), 305–316; DOI: 10.1177/036354659101900317
10. R. Nisell, G. Németh, and H. Ohlsén; Joint forces in extension of the knee: Analysis of a mechanical model; *Acta Orthop.*, 1986, 57(1), 41–46; DOI: 10.3109/17453678608993213
11. V. Guruguntla, M. Lal; A state-of-the-art review on biomechanical models and biodynamic responses; *Ergonomics*, 2025, 68(1), 63–84; DOI: 10.1080/00140139.2023.2288544
12. J. W. Chow; Knee joint forces during isokinetic knee extensions: A case study; *Clin. Biomech.*, 1999, 14(5), 329–338; DOI: 10.1016/S0268-0033(98)00083-7
13. G. T. Yamaguchi, F. E. Zajac; A planar model of the knee joint to characterize the knee extensor mechanism; *J. Biomech.*, 1989, 22(1), 1–10. DOI: 10.1016/0021-9290(89)90179-6
14. Z. Ding, C. K. Tsang, D. Nolte, A. E. Kedgley, A. M. J. Bull; Improving Musculoskeletal Model Scaling Using an Anatomical Atlas: The Importance of Gender and Anthropometric Similarity to Quantify Joint Reaction Forces; *IEEE Trans. Biomed. Eng.*, 2019, 66(12), 3444–3456; DOI: 10.1109/TBME.2019.2905956
15. T. Piontek, K. Ciemniewska-Gorzela, M. Słomczykowski, R. Jakob; All-arthroscopic technique of biological meniscal tear therapy with collagen matrix.; *Polish Orthop. Traumatol.*, 2012, 31(77), 39–45.
16. S. D. Masouros, A. M. J. Bull, A. A. Amis; (i) Biomechanics of the knee joint; *Orthop. Trauma*, 2010, 24(2), 84–91; DOI: 10.1016/j.mporth.2010.03.005
17. K. M. Varadarajan, T. J. Gill, A. A. Freiberg, H. E. Rubash, G. Li; Patellar tendon orientation and patellar tracking in male and female knees; *J. Orthop. Res.*, 2010, 28(3), 322–328; DOI: 10.1002/jor.20977
18. H.Y. Kim et al.; Screw-home movement of the tibiofemoral joint during normal gait: Three-dimensional analysis; *CiOs*, 2015, 7(3), 303–309; DOI: 10.4055/cios.2015.7.3.303
19. J.W. Jeon, J. Hong; Comparison of screw-home mechanism in the unloaded living knee subjected to active and passive movements; *BMR*, 2021, 34(4), 589–595; DOI: 10.3233/BMR-200110
20. B. D. Beynnon et al.; Geometric profile of the tibial plateau cartilage surface is associated with the risk of non-contact anterior cruciate ligament injury; *J. Orthop. Res.*, 2014, 32(1), 61–68; DOI: 10.1002/jor.22434
21. R. Śliwowski, M. Grygorowicz, R. Hojszyk, Ł. Jadczyk; The isokinetic strength profile of elite soccer players according to playing position; *PLoS One*, 2017, 12(7), e0182177; DOI: 10.1371/journal.pone.0182177
22. W. Qi, A. Hosseini, T. Y. Tsai, J. S. Li, H. E. Rubash, G. Li; In vivo kinematics of the knee during weight bearing high flexion; *J. Biomech.*, 2013, 46(9), 1576–1582; DOI: 10.1016/j.jbiomech.2013.03.014
23. P. de Leva; Adjustments to Zatsiorsky-Seluyanov’s segment inertia parameters; *J. Biomech.*, 1996, 29(9), 1223–1230; DOI: 10.1016/0021-9290(95)00178-6
24. L. McCann, E. Ingham, Z. Jin, J. Fisher; Influence of the meniscus on friction and degradation of cartilage in the natural knee joint; *Osteoarthr. Cartil.*, 2009, 17(8), 995–1000; DOI: 10.1016/j.joca.2009.02.012
25. K. B. Shelburne, M. G. Pandy, F. C. Anderson, M. R. Torry; Pattern of anterior cruciate ligament force in normal walking; *J. Biomech.*, 2004, 37(6), 797–805, DOI: 10.1016/j.jbiomech.2003.10.010
26. C. B. Ruff et al.; Stature and body mass estimation from skeletal remains in the European Holocene; *Am. J. Phys. Anthropol.*, 2012, 148(4), 601–617, DOI: 10.1002/ajpa.22087
27. G. Li, K. Kawamura, P. Barrance, E. Y. S. Chao, K. Kaufman; Prediction of Muscle Recruitment and Its Effect on Joint Reaction Forces during Knee Exercises; *Ann. Biomed. Eng.*, 1998, 26(4), 725–733; DOI: 10.1114/1.104
28. R. Nisell, M. O. Ericson, G. Nemeth, J. Ekholm; Tibiofemoral joint forces during isokinetic knee extension; *Am. J. Sports Med.*, 1989, 17(1), 49–54; DOI: 10.1177/036354658901700108
29. N. Petrone, M. Nardon, G. Marcolin; Prediction of ACL and PCL Loads During Isokinetic Knee Exercises using Experimental Tests and Musculoskeletal Simulations; *Procedia Eng.*, 2016, 147, 246–251; DOI: 10.1016/j.proeng.2016.06.251
30. J. Ke et al.; Blood flow restriction training promotes functional recovery of knee joint in patients after arthroscopic partial meniscectomy: A randomized clinical trial; *Front. Physiol.*, 2022, 13; DOI: 10.3389/fphys.2022.1015853
31. R. D. Komistek, T. R. Kane, M. Mahfouz, J. A. Ochoa, D. A. Dennis; Knee mechanics: a review of past and present techniques to determine in vivo loads; *J. Biomech.*, 2005, 38(2), 215–228, DOI: 10.1016/j.jbiomech.2004.02.041

32. R. F. Escamilla; Knee biomechanics of the dynamic squat exercise; *Med. Sci. Sports Exerc.*, 2001, 127–141; DOI: 10.1097/00005768-200101000-00020
33. D. D. D’Lima, S. Patil, N. Steklov, C. W. Colwell; The 2011 ABJS Nicolas Andry Award: ‘Lab’-in-a-Knee: In Vivo Knee Forces, Kinematics, and Contact Analysis; *Clin. Orthop. Relat. Res.*, 2011, 469(10), 2953–2970; DOI: 10.1007/s11999-011-1916-9
34. S. L.-Y. Woo, J. M. Hollis, D. J. Adams, R. M. Lyon, S. Takai; Tensile properties of the human femur-anterior cruciate ligament-tibia complex; *Am. J. Sports Med.*, 1991, 19(3), 217–225, DOI: 10.1177/036354659101900303
35. M. A. Wimmer, T. P. Andriacchi; Tractive forces during rolling motion of the knee: Implications for wear in total knee replacement; *J. Biomech.*, 1997, 30(2), 131–137; DOI: 10.1016/S0021-9290(96)00112-1
36. E. Kellis; Tibiofemoral joint forces during maximal isokinetic eccentric and concentric efforts of the knee flexors; *Clin. Biomech.*, 2001, 16(3), 229–236; DOI: 10.1016/S0268-0033(00)00084-X
37. R. F. Escamilla, T. D. Macleod, K. E. Wilk, L. Paulos, J. R. Andrews; ACL Strain and Tensile Forces for Weight Bearing and Non—Weight-Bearing Exercises After ACL Reconstruction: A Guide to Exercise Selection; *J. Orthop. Sport. Phys. Ther.*, 2012, 42(3), 208–220; DOI: 10.2519/jospt.2012.3768
38. D. L. Butler, F. R. Noyes, E. S. Grood; Ligamentous restraints to anterior-posterior drawer in the human knee. A biomechanical study.; *J. Bone Joint Surg. Am.*, 1980, 62(2), 259–70

© 2025 by the Authors. Licensee Poznan University of Technology (Poznan, Poland). This article is an open access article distributed under the terms and conditions of the Creative Commons Attribution (CC BY) license (<http://creativecommons.org/licenses/by/4.0/>).